LWT - Food Science and Technology 96 (2018) 568–575

Contents lists available at ScienceDirect

LWT - Food Science and Technology

journal homepage: www.elsevier.com/locate/lwt

Development and characterization of maltodextrin microparticles to encapsulate heme and non-heme iron

Osmaly Churio, Carolina Valenzuela*

Faculty of Veterinary and Animal Sciences, University of Chile, Av. Santa Rosa 11735, La Pintana, Santiago, 8820000, Chile

ARTICLE INFO

Keywords:
Encapsulation
Iron
Maltodextrin
Spray-drying

ABSTRACT

Selection of an appropriate encapsulating material and its properties are critical issues to optimize iron encapsulation systems. Therefore, the aim of this work was to develop and characterize different types of heme and non-heme iron-maltodextrin microparticles. Different concentrations of bovine erythrocytes (BE) and ferrous sulfate (FS) were encapsulated using an optimal maltodextrin concentration of 40% w/v by spray-drying. The microparticles were characterized by iron content, yield, Z potential, size, color, SEM, FTIR and iron release under simulated gastrointestinal conditions. Results indicate that FS microparticles exhibited a higher iron content (54–90 mg/g) than BE microparticles (0.28–0.77 mg/g), Z Potential for all microparticles was negative and FS microparticles had a smaller size (918–981 nm) than BE microparticles (10,390–16,643 nm). FS microparticles had an irregular spherical shape and a shriveled surface, while BE microparticles exhibited a spherical shape and a smooth surface. The main interactions of FS microparticles were O–H bridges and C–O bonds, whereas for BE microparticles these were O–H, C–O and N–H bonds. Iron was released from both types of microparticles: high amounts under gastric conditions, and quickly under intestinal conditions.

1. Introduction

Iron-deficiency anemia is the most common nutritional deficit worldwide, affecting up to one third of the population (World Health Organization, 2015). One of its main causes is poor dietary intake of heme iron (De Benoist, McLean, Egli, & Cogswell, 2008), because heme iron sources from meat products are expensive and not available for a sizable part of people in developing countries.

Oral iron supplementation has been attempted, though it presents some disadvantages due to several factors, such as its poor organoleptic properties, low iron bioavailability from non-heme sources currently being used, and the inconvenience of requiring multiple, high concentration doses to achieve a therapeutic goal (Viteri, 1997; Zimmermann & Hurrell, 2007). All of these issues can be reduced by using an encapsulation technology for iron supplements and iron-fortified products, as it has been evidenced by several accounts of good results when it is used in human and animal studies (Tondeur et al., 2004; Xu et al., 2014; Yuan et al., 2013). Most studies have tested iron encapsulation systems based on liposome technology (Tondeur et al., 2004; Zimmermann, 2004), which uses several kinds of encapsulating materials: phospholipids (from different sources), cholesterol, lecithin, and emulsifiers such as tween (Ding et al., 2011; Xu et al., 2014; Yuan et al., 2013). But liposomes are not recommended for oral supplementation due to their low encapsulation efficiency (Yuan et al., 2013), the elevated cost of both materials and devices required for their manufacture (Nedovic, Kalusevic, Manojlovic, Levic, & Bugarski, 2011), and also because of their thermodynamic instability – which results in quick degradation under intestinal conditions and the release of their nucleus material (Kokkona, Kallinteri, Fatouros, & Antimisiaris, 2000). Other materials and methods that have been studied to determine their suitability for encapsulating iron are: sodium alginate by ionic gelation (Churio, Pizarro, & Valenzuela, 2018; Perez-Moral, Gonzalez, & Parker, 2013; Valenzuela, Hernández, Morales, & Pizarro, 2016; Valenzuela, Hernández, Morales, Neira-Carrillo, & Pizarro, 2014), vegetable oils, fatty acids and polyglycerols by emulsions (Choi, Decker, & Mc Clements, 2009; Zariwala et al., 2013; Zimmermann, 2004), cellulose-derived polymers and gum/carbohydrate blends by extrusion or solvent evaporation (Gupta, Chawla, Arora, Tomar, & Singh, 2015; Li, Diosady, & Wesley, 2010).

Absorption of encapsulated iron supplements has been improved by combining non-heme iron with heme iron sources (Yuan et al., 2013), as the latter not only exhibits a higher bioavailability but it also maximizes non-heme absorption (Carpenter & Mahoney, 1992; Conrad & Umbreit, 2002; Lipiński, Stys, & Starzyński, 2013). This potentiating effect is specially marked when whole-erythrocytes are used in a formulation (Pizarro et al., 2016).

* Corresponding author. Casilla 2 correo 15 La Granja, Santiago, Chile.
E-mail addresses: osmaly@veterinaria.uchile.cl (O. Churio), cvalenzuelav@u.uchile.cl (C. Valenzuela).

https://doi.org/10.1016/j.lwt.2018.05.072
Received 5 February 2018; Received in revised form 29 May 2018; Accepted 31 May 2018
Available online 31 May 2018
0023-6438/

Maltodextrins are polymer products from the hydrolysis of starch. These polymers are composed by α-D-glucopyranosyl residues that are linked by α-1,4-bonds, and arranged as linear chains with branching points links at a degree of (1 → 4, 1 → 6) or (1 → 6) (Chronakis, 1998). Choosing maltodextrins as an encapsulating material presents several advantages, such as its low cost and wide availability in the market, its reduced viscosity, its ample compatibility with different materials (Kenyon, 1995), and its compatibility with spray-drying technology. The latter is specially relevant, as it is the most common technology currently being used in the food industry due to its low cost and readily available equipment (Gharsallaoui, Roudaut, Chambin, Voilley, & Saurel, 2007). While several studies have used maltodextrin to manufacture microparticles for a great range of nucleus materials (Cai & Corke, 2000; Kenyon, 1995), not much research has been done on their use as encapsulating agents for oral iron supplementation in humans. To the extent of our knowledge, the only work that used maltodextrin to encapsulate iron did so using a mixture of maltodextrin, arabic gum and modified starch (Gupta et al., 2015).

Finally, encapsulation technology could allow using two different iron sources and enhancing their absorption, as well as protecting them during their passage through the gastrointestinal tract and favoring a greater iron bioavailability than in non-encapsulated iron supplements. Therefore, the aim of this work was to manufacture and characterize different types of heme and non-heme iron-maltodextrin microparticles.

2. Materials and methods

2.1. Material

Food–grade maltodextrin (20 Dextrose Equivalent) was chosen for the encapsulating material, whereas for the nucleus of the microparticles ferrous sulfate (FS) heptahydrate was the non-heme iron source and atomized bovine erythrocytes (BE) were the heme iron source. These materials were sourced from Prinal S.A. (Santiago, Chile), Merck® (Merck KGaA, Darmstadt, Germany), and Licán Alimentos S.A. (Santiago, Chile), respectively. Considering the risks associated to the use of bovine erythrocytes for animal feeding purposes, Licán Alimentos S.A. were chosen to provide this product as their procedures follow international quality standards, such as HACCP Codex Alimentarius, GMP, and ISO 9001:2008-UKAS.

Total iron content for FS and BE was determined by using a GBC 905AA atomic absorption spectrophotometer (GBC Scientific Equipment, Braeside, Australia) following directives 999.11 (AOAC, 1996) for the method of acid digestion. Spectrophotometric measurements were then assessed against a standard curve plotted at a wavelength (λ) of 248.3 nm for a 1000 μg/mL commercial iron standard solution (J.T. Baker, USA).

Pepsin from porcine gastric mucosa (Sigma–Aldrich, USA), porcine pancreatin (Sigma–Aldrich, USA) and porcine bile extract (Sigma–Aldrich, USA), were used to perform an *in vitro* simulation of normal gastrointestinal conditions.

2.2. Iron–microparticles elaboration

Several maltodextrin solutions were prepared in deionised water at different concentrations (10, 20, 30, and 40% w/v), and then subjected to a rotational viscosity test at 25 °C using a digital viscometer (Brookfield Engineering Laboratories, Inc., Stoughton, USA) with a N°61 spindle. FS and BE were then dispersed in maltodextrin solutions using a magnetic stirrer. These solutions were prepared at different concentrations: 10, 20, 30 and 40% w/v for FS, and 5, 10, 15 and 20% w/v for BE. Afterward, the rotational viscosity of higher concentration blends was determined for each nucleus material.

Homogenized blends were then immediately fed to a B–290 Mini Spray Dryer (BÜCHI Labortechnik AG, Flawil, Switzerland). As for the operational parameters, the inlet and outlet air temperatures were set at 140 ± 5 °C and 95 ± 5 °C, respectively. The air flow, rate of feeding and atomization pressure were 500 L/h, 8 mL/min and 20 psi, respectively.

The resulting spray–dried powder for every blend was collected in plastic recipients and stored at room temperature within desiccators which contained silica gel. Then, samples from each blend were observed by Scanning Electron Microscopy (SEM). These samples were mounted on a cylindrical aluminum stub using double–sided tape to sputter coat them with gold, twice, at 20 kV in an argon atmosphere by a PELCO 91000 sputter coater unit (Ted Pella, Inc., Redding, California). Coated samples were then examined on a LEO 1420 VP scanning electron microscope (LEO Electron Microscopy, Cambridge, UK) at an accelerating voltage of 25 kV. According to this SEM examination, all those blends whose spray–dried powder samples did not form microparticles were discarded.

2.3. Iron–microparticles characterization

2.3.1. Color and appearance

The spray–dried powder was photographed using a Sony DSC–HX1 digital camera (Sony corporation, Japan) to observe the appearance of each blend, and their color profile parameters on the Hunter Lab color scale were measured using a Konica–Minolta CR–300 colorimeter (Konica–Minolta, Inc., Japan).

2.3.2. Iron content, yield and iron retention

Iron content in microparticles was determined using atomic absorption, calculating iron yield following both the methodology and equation proposed by Castro, Barragán, and Yáñez (2015). Equation (1) presents production yields as the weight percentage of the final product relative to the total amount of sprayed materials.

$$Y\% = \frac{Wf}{Wi} \times 100 \quad (1)$$

Where Y is the yield percentage, Wf is the weight of spray–dried powder (g) and Wi is the initial weight of non–solvent materials fed to the spray dryer.

Iron retention (IR) was calculated as the ratio of actual iron in powder of a spray–dried blend, in relation to the theoretical iron content of the blend materials that were fed to the spray dryer unit (Equation (2)).

$$IR = \frac{AI}{TI} \times 100 \quad (2)$$

Where AI is the actual iron and TI is the theoretical iron.

2.3.3. Particle size and zeta potential

The size distribution for each microparticle was determined using a laser light diffraction instrument (Brookhaven Instrument Corp., USA). Zeta potential in maltodextrin, FS, BE and microparticles was measured using a Zeta Plus zeta analyzer instrument from Brookhaven instruments Corporation (New York, USA).

2.3.4. Fourier transform infrared spectroscopy (FTIR)

The structural characterization of microparticles, as well as from their nucleus (FS and BE), and maltodextrin was completed by performing a Fourier transform infrared spectroscopy (FTIR) analysis, using an ATR/FTIR Interspec 200–X spectrometer (Interspectrum OU, Estonia). A PIKE Miracle™ accessory in a single–reflection Germanium crystal plate allowed performing direct spectroscopic measurements of all samples. A concave tip was used in all FTIR spectra analyses, which represented the average of 30 scans over the 500–4000 cm^{-1} wavelength range.

2.4. In vitro iron release studies

Gastric and intestinal conditions were simulated *in vitro* following a method described by Churio et al. (2018). For the gastric conditions simulation, a base solution was prepared dissolving 1 mol/L of a pepsin solution in 25 mol/L of PBS buffer (0.l M, pH 6.0) and then adding HCl 1N to adjust its pH down to 2.0. This pepsin solution contained 25 mg of pepsin. Next, 1 g of microparticles was mixed with 100 mol/L of this suspension and incubated them for 1 h at 37 °C under constant agitation (150 oscillations/min).

To simulate intestinal conditions, the following components were added to the solution above: 10 g/L of pancreatin, 31.2 g/L of bile extract, PBS buffer solution and HCl 1N as necessary to adjust its pH down to 6.0. Like before, this solution was also kept at 37 °C under constant agitation (150 oscillations/min), but this time it was incubated for 2.5 h.

At each simulation 5 mol/L aliquots were sampled from either suspension, every 15 min, to measure total iron release from these microparticles. Measurements were performed via atomic absorption spectroscopy analysis.

2.5. Statistical analysis

Statistix® 8 software package (Analytical Software 2003, Tallahassee, FL) was used for all statistical analyses. The assays were subjected to ANOVA, and means comparisons were adjusted by Tukey ($P < 0.05$).

3. Results and discussion

3.1. Microparticles development

Every solution prepared had viscosity values that were amenable for spray drying atomization. For maltodextrin solutions viscosity ranged between 11.8 and 30.0 mPa·s, while for blends of FS (40% FS with different maltodextrin concentrations) it ranged from 24.0 to 82.1 mPa·s. On the other hand, 20% BE blends had notoriously greater viscosity values ranging from 62.8 to 183.6 mPa·s due to the gelification effect of hemoglobin on dispersions (Valenzuela et al., 2014). Unsurprisingly, increasingly concentrated maltodextrin solutions became significantly more viscous, which is consistent with reports from other authors (Dokic, Jakovljevic, & Dokic-Baucal, 1998).

Based on microphotographs from spray–dried powder for the different blends (Fig. 1), those blends containing only 10% (not shown in Figs. 1) and 20% maltodextrin (Fig. 1A and B) were discarded as they were unable of forming microparticles for any type of nucleus material. The results found for microparticles that were created from blends with higher concentrations of maltodextrin indicated that, as the encapsulating material increased, these were proportionally better formed. Amorphous structures were found on 20% maltodextrin solutions. These structures were characterized by an heterogeneous composition, agglomerating and forming bridges, for both types of nucleus materials. This finding agrees with previous reports about observing similar microstructures for maltodextrin when it has been used as an encapsulating material, at low concentration levels, in spray drying methods (Cano-Chauca, Stringheta, Ramos, & Cal-Vidal, 2005; Mishra, Mishra, & Mahanta, 2014). Beginning with 30% maltodextrin solutions, we noticed that those solutions prepared with BE did form some microparticles (Fig. 1D), though these microparticles were quite heterogeneous regarding their size and shape. On the other hand, those solutions that were prepared with FS (Fig. 1C) still produced similar structures to those described above (Fig. 1A and B).

Microparticles finally became well formed when using 40% maltodextrin solutions, for both FS and BE nucleus materials. This maltodextrin concentration is higher than what other authors have used to encapsulate food ingredients using spray-drying methods (Cano-Chauca et al., 2005; Santiago et al., 2015). However, high concentrations were also used in the nucleus material of these microparticles. The reason behind this decision was the consideration that, in the future, this microparticles might have an application as supplements or in food fortification strategies, as the non-heme form of iron widely interacts with other diet components. These interactions mean its inhibition, precipitation, and competition with other minerals to be absorbed in the digestive system (Conrad & Umbreit, 2002). Thus, fortified foods and supplements must use high concentrations of this micronutrient to fulfill its purpose.

FS microparticles were shaped as irregular spheres with a dented and shriveled surface (Fig. 1E), which is regarded as a typical morphology for maltodextrin spray–dried powder (Cai & Corke, 2000; Di Battista, Constenla, Ramírez-Rigo, & Piña, 2015). In this regard, Loksuwan (2007) reported that rugosity and concavities in their microparticles resulted from shrinkage as their surfaces dried up. BE microparticles, in turn, exhibited a spherical shape and a smooth surface (Fig. 1F). This finding was not an unexpected development though, as it has been previously reported that some materials have a plasticizing effect that reduces coarseness on the surface of polysaccharides microparticles. This effect could be explained as BE presents protein concentration levels that are close to 90% (Valenzuela et al., 2014), conferring it great hygroscopic power, similarly to what has been reported for hydrolyzed meat extracts, whose microparticles also present a smooth surface (Kurozawa, Park, & Hubinger, 2009).

Based on these findings, 8 types of microparticles were characterized. All of them were assigned a fixed concentration level of encapsulating material (40% maltodextrin), and four different FS and BE concentration levels.

3.2. Microparticles characteristics

3.2.1. Appearance

Fig. 1 shows some types of spray–dried powder. Those containing FS displayed no color differences in spite of increasing FS concentration levels (Fig. 1A, C and E; also Table 1), unlike those containing BE, whose color turned to increasingly darker shades of reddish–brown (Fig. 1B, D and F; also Table 1), which is proper of BE itself. On the other hand, the naturally turquoise color of FS in its pure state, rendered spray–dried powder blends within a narrow range of pale green shades.

3.2.2. Iron content, yield and iron retention

As expected, FS microparticles had a high iron content resulting from its non-heme iron source, which provides 179 ± 5 mg of iron per gram of FS. This situation contrasted with BE microparticles, whose iron content was lower due to BE providing only 2.49 ± 0.07 mg of iron per gram of BE. Also, increasing the concentration of nucleus material resulted in significant increments in iron content for all microparticles (Table 1). The evident disparity in iron content of microparticles is a consequence of iron sources themselves. Inorganic sources present higher iron concentration because these are iron salts, whereas organic heme-iron sources are contained within erythrocytes or in hemoproteins, such as hemoglobin, myoglobin, and cytochromes (Ponka, 1999).

Producing BE microparticles is highly relevant in spite of their low iron contribution, as 99 percent of BE iron is found as part of the heme group (Valenzuela et al., 2014). This confers BE microparticles several advantages, such as: 1) Heme iron bioavailability is quite superior (15–35%) to non-heme iron (1–20%) (Carpenter & Mahoney, 1992; Conrad & Umbreit, 2002). 2) Humans absorb iron mainly in the duodenum, by different pathways and through different receptors, depending on whether it is heme iron (proton–coupled folate transporter/heme carrier protein 1, PCFT/HCP1) or non-heme iron (divalent metal transporter 1, DMT1) (Conrad & Umbreit, 2002; Lipiński et al., 2013). 3) It has been reported a greater expression of genes that are related to

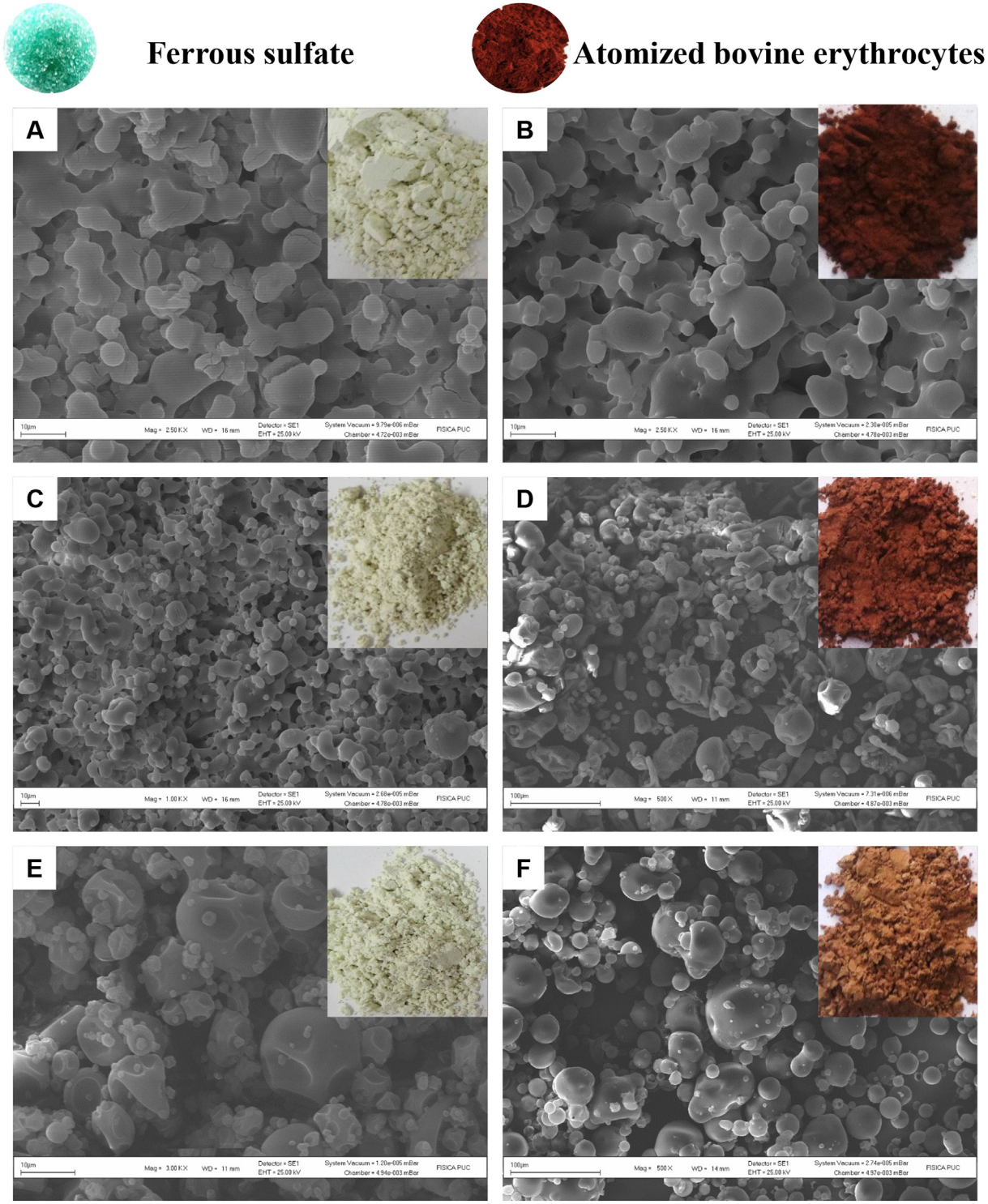

Fig. 1. SEM and digital images of some ferrous sulfate and atomized bovine erythrocytes spray-dried powders. Each row corresponds to solutions of maltodextrin at different concentration. A and B: 20%. C and D: 30%. E and F: 40%.

absorption of heme iron (HCP1) and transport (Heme-binding protein, HRG–1) (Conrad & Umbreit, 2002; Lipiński et al., 2013). 4) Heme iron has a potentiating effect over the absorption of non-heme iron (Conrad & Umbreit, 2002). 5) Heme iron is also the least consumed form of iron by anemic population in developing countries (Carpenter & Mahoney, 1992).

The maximum concentration of BE used in this work was 20% w/v, due to encapsulation technology reasons. Higher concentrations result in overly viscous dispersions (data not shown) that hardly pass through the atomization equipment, even to the point of risking clogging its nozzles. Other studies have used water-soluble heme trying to encapsulate higher concentrations of heme iron (Yuan et al., 2013). However, in a recent study on humans, Pizarro et al. (2016) described that bioavailability of water-soluble heme ranged from 10 to 13%, which is less than half the bioavailability found in whole-erythrocytes (25%).

The iron concentration observed in 20% BE microparticles was similar to what Valenzuela et al. (2014) reported for BE–alginate beads

Table 1
Iron content, iron yield, iron retention (IR), Z potential (Z), size and color for different types of microparticles at several iron concentration levels.

Types	Content (mg/g)	Yield (%)	IR (%)	Z (mv)	Size (nm)	Color		
						L	*a*	*b*
FS 10%	54.0 ± 0.3^{a}	52 ± 6^{a}	88 ± 6^{a}	−9.8 ± 1.5^{a}	918 ± 17^{a}	59.7 ± 0.6^{a}	59.7 ± 0.6^{a}	59.7 ± 0.6^{a}
FS 20%	66.5 ± 0.7^{b}	53 ± 4^{a}	83 ± 8^{a}	−10.1 ± 0.4^{a}	933 ± 28^{a}	60.6 ± 0.6^{a}	60.6 ± 0.6^{a}	60.6 ± 0.6^{a}
FS 30%	78.4 ± 1.1^{c}	57 ± 4^{a}	83 ± 4^{a}	−12.6 ± 1.0^{b}	959 ± 17^{b}	60.6 ± 2.5^{a}	60.6 ± 2.5^{a}	60.6 ± 2.5^{a}
FS 40%	90.3 ± 1.1^{d}	54 ± 4^{a}	88 ± 8^{a}	−12.3 ± 1.6^{b}	981 ± 7^{c}	59.1 ± 2.9^{a}	59.1 ± 2.9^{a}	59.1 ± 2.9^{a}
BE 5%	0.28 ± 0.09^{e}	47 ± 5^{b}	87 ± 5^{a}	−4.1 ± 0.6^{c}	10.390 ± 159^{d}	13.7 ± 0.2^{b}	13.7 ± 0.2^{b}	13.7 ± 0.2^{b}
BE 10%	0.42 ± 0.10^{f}	45 ± 3^{b}	85 ± 5^{a}	−3.9 ± 0.2^{c}	11.670 ± 155^{e}	15.1 ± 0.1^{c}	15.1 ± 0.1^{c}	15.1 ± 0.1^{c}
BE 15%	0.65 ± 0.08^{g}	44 ± 4^{b}	83 ± 12^{a}	−3.7 ± 0.4^{c}	14.429 ± 330^{f}	18.3 ± 1.0^{d}	18.3 ± 1.0^{d}	18.3 ± 1.0^{d}
BE 20%	0.77 ± 0.11^{h}	39 ± 2^{c}	81 ± 7^{a}	−4.4 ± 0.8^{c}	16.643 ± 261^{g}	20.3 ± 0.4^{e}	20.3 ± 0.4^{e}	20.3 ± 0.4^{e}

Means with different superscript letters present significant statistical differences ($P < 0.05$).

(0.658 mg of iron/g of beads). Meanwhile, iron content for FS microparticles was lower than what was reported for microcapsules containing an FS core and walls made from an arabic gum:maltodextrin:modified starch (4:1:1 ratio) mixture (Gupta et al., 2015). These microcapsules delivered 300 mg of iron per gram, though is worth noting that Gupta et al. (2015) used higher concentrations of FS than those used in this work.

High iron retention values that were similar for all microparticles were found by the end of the encapsulation process. An expected outcome though, as iron is quite stable when it is exposed to high temperatures. Regarding iron yield, results indicated that FS microparticles had a higher yield than BE microparticles (Table 1), and that those microparticles with 20% of BE had an even lower yield than the rest of the microparticle blends. The yield range observed for microparticles used in this work was in line with reports from other authors, who also developed maltodextrin microparticles by a spray drying technique but using different materials within their nucleus (Santiago et al., 2015; Tonon, Brabet, & Hubinger, 2008). In the case of BE microparticles, a possible reason for such a lower yield might be that, as those blends had greater viscosity, a higher amount of solids remained attached to the walls of the drying chamber (Tonon et al., 2008).

3.2.3. Z potential and size

When calculating the Z potential for both the materials and microparticles. In particular, materials Z potential values were +29.8 ± 5.1, −20.3 ± 7.4, and −3.4 ± 0.2 for maltodextrin, FS, and BE, respectively. Z potential was negative for all microparticles (Table 1), though it was less negative for BE microparticles due to the contribution of their BE nucleus material, as detailed above. BE microparticles presented no significant differences among them, whereas FS microparticles showed Z potential values that became increasingly more negative as FS concentrations increased up to 30% of the blend. This may be explained by the presence of sulfate –type anionic groups in the structure of FS, which confer it an intrinsically negative charge (Thielbeer, Donaldson, & Bradley, 2011). It could also contribute to this results that FS might become superficially trapped on its microparticles (matrix ordering). The same mechanism could also occur in BE microparticles.

As for particle size, FS microparticles were found to be smaller than BE microparticles (Table 1), and particle size increased proportionally with the concentration of their nucleus material, as expected. Meanwhile, the size of BE microparticles could be explained by the greater viscosity observed in the blend solutions that were used to prepare these microparticles (Tonon et al., 2008; Wichchukit, Oztop, McCarthy, & McCarthy, 2013).

3.2.4. FTIR spectroscopy

FTIR spectroscopy was used to confirm that FS and BE solutions were successfully encapsulated within maltodextrin microparticles. Fig. 2 presents FTIR values for microparticles, as well as for their nucleus and wall materials. Fig. 2A shows bands that are typical for maltodextrin, FS, and BE. Maltodextrin shows a strong band at 3337 cm^{-1}, which is characteristic for hydroxyl (O–H) groups (Santiago et al., 2015), and it is present in all microparticles as well. However, for BE microparticles this band is sharper (Fig. 2C) than for FS microparticles (Fig. 2B), due to BE also having a strong, sharp band in the area of O–H groups. Another important band for maltodextrin is located at 1024 cm^{-1}, which represents C–O bonds stretching vibrations (Santiago et al., 2015), and it seems to be quite similar for 10% FS microparticles, as well as for 5% BE microparticles. However, as FS concentration levels increased, this band resembled another band that is located at 1081 cm^{-1}, within the spectra of FS. Meanwhile, though this band remained structurally akin to the one observed in the spectra of maltodextrin, this band became shorter for the concentration of 15% BE. This finding would indicate that C–O bond interactions became less relevant for this type of microparticles.

FS microparticles seemed to preserve much of the structure from its constituent materials, even to the point that increasing the concentration of FS resulted on the microparticles spectra progressively resembling the spectrum of pure FS. Even a small spectral band (1625 cm^{-1}), that represents C = O bond interactions, remained present.

Other BE spectral bands showed that BE was present within its microparticles. For example, the band located at 2963 cm^{-1} represents C–H bond stretching interactions, which are characteristic of BE (Valenzuela et al., 2014). Furthermore, a spectral band that represent C–O bond stretching vibrations from amide I was also found at 1650 cm^{-1}, as well as another band at 1542 cm^{-1}, which is evidence of N–H bond bending vibrations from amide II (Valenzuela et al., 2014). As expected, these bands became more prominent as BE concentration increased in these microparticles.

Based on these results encapsulation presumably did occur for FS and BE, as these data are consistent with previous observations from Santiago et al. (2015), regarding maltodextrin microparticles that these researchers developed to encapsulate cinnamon infusions.

3.3. In vitro studies

Fig. 3 presents curves for the release of iron from microparticles, during an *in vitro* simulation of gastrointestinal conditions. The amount of iron released from these microparticles was expressed as the percentage of total iron contained within each type of microparticle. According to what was found after simulating gastric conditions, BE microparticles released less iron than FS microparticles over the whole incubation period. Specifically, by the end of the simulation, BE microparticles released iron in a range of 20.9%–22.7%, while FS microparticles released it in a range of 31.8%–37.4%. The latter roughly represented one third of the total iron content of the different FS microparticles. Also, the amount of nucleus material in microparticles of the same type did not affect their iron release pattern.

Under simulated intestinal conditions, the iron release behavior of BE microparticles and FS microparticles presented significant differences during the first 45 min of incubation. At this point in time, BE

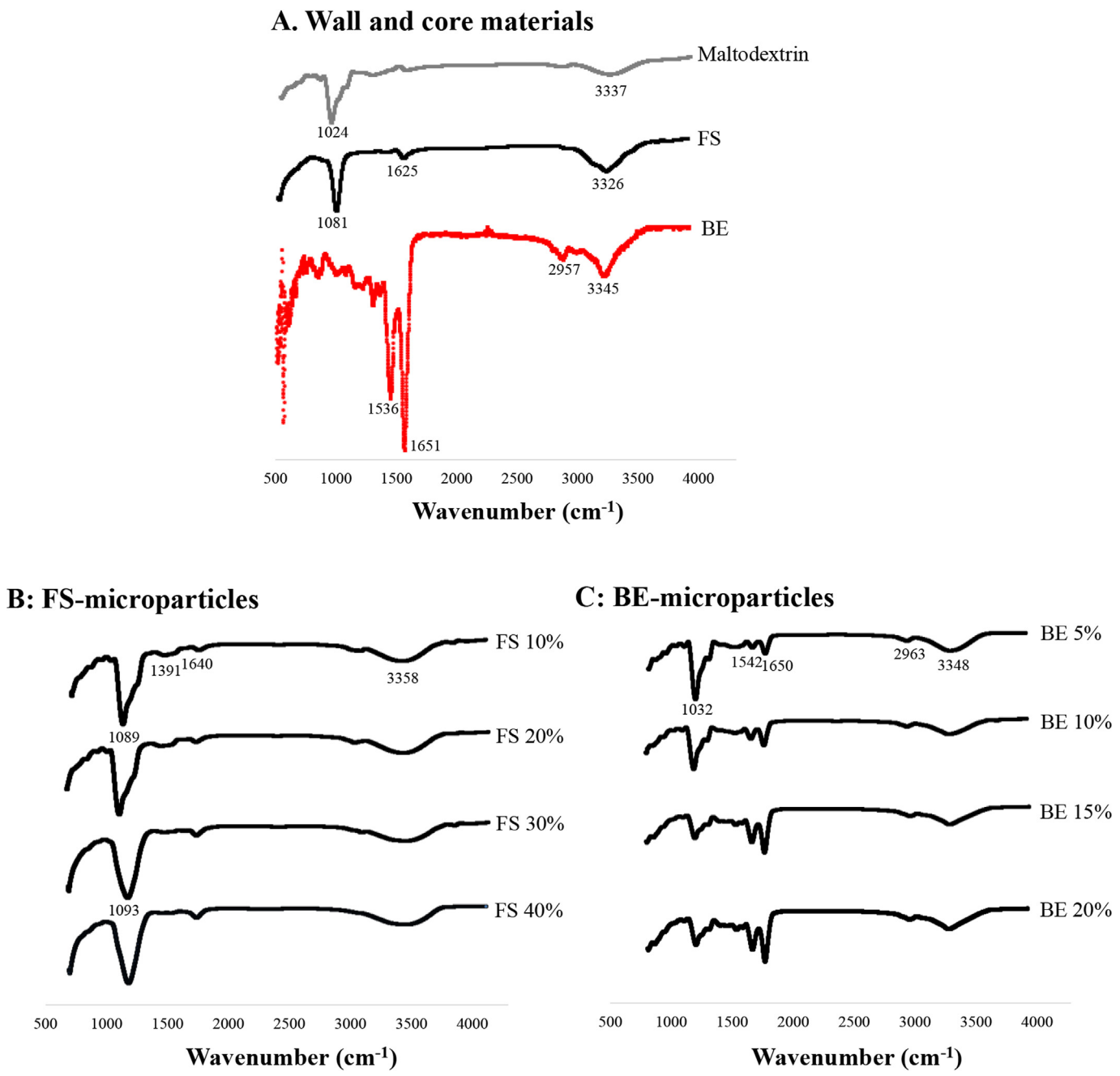

Fig. 2. FTIR spectra for: (A) wall and core materials, (B) Ferrous sulfate (FS) microparticles and (C) atomized bovine erythrocytes (BE) microparticles.

microparticles released less iron than FS microparticles. By the end of the incubation period though, both types of microparticles had released close to 100% of their iron content. It is also worth noting that both types of microparticles differed regarding the speed of iron release. In particular, after 30 min of incubation (minute 90 in Fig. 3), FS microparticles released close to 80–85% of their iron content, whereas BE microparticles had only released 65–68% of it. Thirty minutes later (minute 120 in Fig. 3), FS microparticles had released close to 90% of its iron content, and BE microparticles reached 83–87%. Any remaining difference disappeared by the end of the incubation period.

These differences regarding the iron release from microparticles could be explained by characteristics that are characteristic to each nucleus material, such as the greater solubility of FS in some solutions. FS solutions also had less viscosity than those with BE, probably resulting in microparticles that could surrender their iron contents more quickly than their counterparts. Also, the FTIR analysis showed different interactions for each type of microparticles, which in turn could exert an effect on their iron release behavior. For example, hydrophobic interactions were observed within the spectrum of BE microparticles (Fig. 2C), and these might lessen the solubility of these microparticles in the incubation media. Additionally, Valenzuela et al. (2016) previously showed that after BE–alginate beads disintegrated, some BE remnants were still present in those beads when they were examined by transmission electron microscopy. This suggests that a similar phenomenon could be at play in the case of BE microparticles, thus contributing to a slower release of iron from these microparticles.

It is difficult though, to properly compare the results of this work in regards to the gastrointestinal release of iron, with those from other studies. Most of those studies used a mixture of maltodextrin with another polymer (Gupta et al., 2015; Lim & Nyam, 2016), whereas in other studies their microparticles had been subjected to non–enzymatic digestion (Santiago et al., 2015; Vergote et al., 2001).

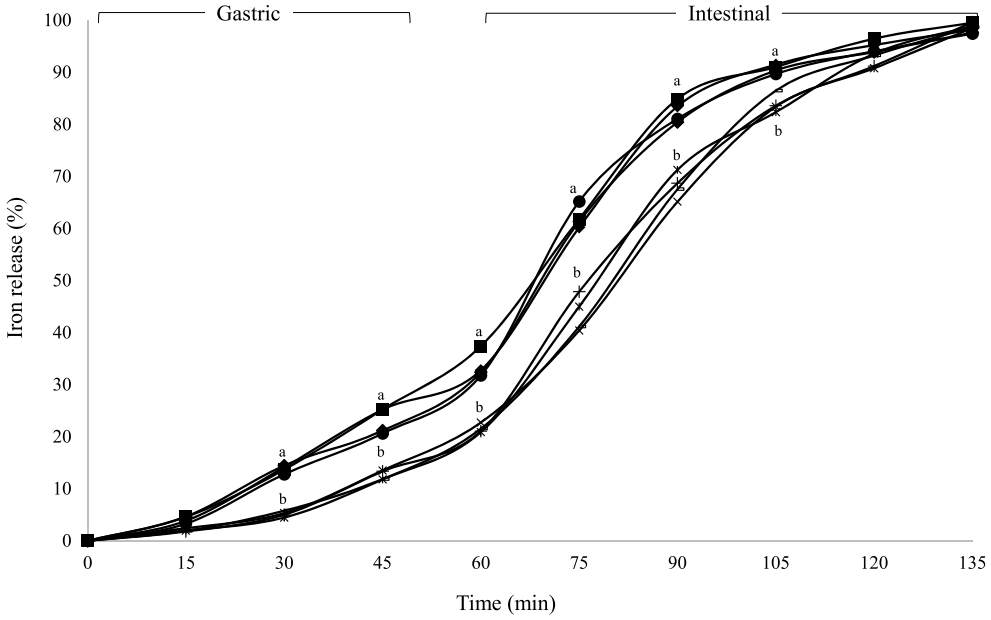

Fig. 3. Cumulative iron release for ferrous sulfate (FS) and atomized bovine erythrocytes (BE) microparticles under gastric and intestinal conditions. Means with different superscript letters present significant statistical differences ($P < 0.05$). Leyends: FS 10% ( ), FS 20% ( ), FS 30% ( ), FS 40% ( ),BE 5% ( ), BE 10% ( ), BE 15% ( ), BE 20% ( ).

In summary, both types of microparticles released vast amounts of iron by the end of the gastric incubation, whereas iron release was characterized by its speed by the end of the intestinal incubation.

A possible explanation for the observations in this work could be that maltodextrin is a polymer that tends to easily scatter and get dissolved in water (Chronakis, 1998; Wang & Wang, 2000). As there is plenty of water within the gastric environment, this factor could account for such a high release of iron at this level. Also, maltodextrin is easily hydrolyzed by human intestinal enzymes due to its chemical composition (it is a polysaccharide), which is characterized by several glucose units that are linked by α–glucosidic bonds (Chronakis, 1998). The simulation of intestinal conditions obviously included those enzymes, henceit is logical to expect such an accelerated iron release during the incubation period.

Currently, liposome entrapment is the most commonly used iron-encapsulation technique. However, liposomes are also unstable under intestinal conditions, due to degradation of their membranes by some enzymes, such as the pancreatic lipase (Kokkona et al., 2000). Notwithstanding such degradation and the high production cost of liposomes (Nedovic et al., 2011), most iron-fortified foods use this encapsulation method (Zimmermann, 2004). Furthermore, this technique was used to prepare renowned products, such as 'Sprinkles' (Zlotkin et al., 2005). These were individual sachets that, among other components, contained ferrous fumarate liposomes and were used by the World Health Organization as a global strategy to reduce iron deficiency anemia in children (http://www.who.int/elena/titles/micronutrientpowder_infants/en/).

Finally, future challenges in this area include reducing iron release under gastric conditions, as well as slowing down its release under intestinal conditions. These aims could be achieved by using double coating to the maltodextrin-microparticles that could be applied either by spray-drying techniques or a fluidized bed. Sodium alginate could be a promising material because its ability of efficiently encapsulating atomized bovine erythrocytes, as well as some inorganic iron salts (Churio et al., 2018; Valenzuela et al., 2014). It can also release low amounts of iron at the gastric level, and then release it at a controlled rate over approximately 2.5 h at the intestinal level (Valenzuela et al., 2016).

4. Conclusions

In this work, high concentrations of both heme and non-heme iron sources were encapsulated within maltodextrin microparticles, in solutions of 40% w/v of maltodextrin. Although iron content of FS microparticles was higher than in BE microparticles, the high bioavailability of heme-iron suggests that a combination of both should be considered for the development of an iron supplement or to fortify food that could be used for the treatment of iron deficiency anemia. Double coating of maltodextrin-microparticles is recommended to improve their iron release behavior under gastrointestinal conditions.

Declaration of conflicts

The authors declare that they have no conflicting financial interests.

Funding

This study was supported by FONDECYT 11140249.

Acknowledgments

Carolina Valenzuela designed this study, performed research tasks and interpreted the data. Osmaly Churio performed research tasks and interpreted the data. Both researchers wrote this manuscript, and Carolina Valenzuela was primarily responsible for the final document, which was approved by every author. We would like to thank Sotiris Chaniotakis for his assistance with the edition of this manuscript.

References

AOAC (1996). *Official methods of analysis of the association of official analytical chemists* (16th ed.). Gaithersburg: AOAC International.

Cai, Y. Z., & Corke, H. (2000). Production and properties of spray-dried amaranthus betacyanin pigments. *Journal of Food Science, 65*, 1248–1252.

Cano-Chauca, M., Stringheta, P. C., Ramos, A. M., & Cal-Vidal, J. (2005). Effect of the carriers on the microstructure of mango powder obtained by spray drying and its functional characterization. *Innovative Food Science & Emerging Technologies, 6*, 420–428.

Carpenter, C. E., & Mahoney, A. W. (1992). Contributions of heme and nonheme iron to human nutrition. *Critical Reviews in Food Science and Nutrition, 31*, 333–367.

Castro, R., Barragán, B. E., & Yáñez, J. (2015). Use of gelatin–maltodextrin composite as an encapsulation support for clarified juice from purple cactus pear (*Opuntia stricta*). *LWT- Food Science and Technology, 62*, 242–248.

Choi, S., Decker, E., & Mc Clements, D. (2009). Impact of iron encapsulation within the interior aqueous phase of water-in-oil-in-water emulsions on lipid oxidation. *Food Chemistry, 116*(1), 271–276.

Chronakis, I. (1998). On the molecular characteristics, compositional properties, and structural–functional mechanisms of maltodextrins: A review. *Critical Reviews in Food Science and Nutrition, 38*, 599–637.

Churio, O., Pizarro, F., & Valenzuela, C. (2018). Preparation and characterization of iron-alginate beads with some types of iron used in supplementation and fortification strategies. *Food Hydrocolloids, 74*, 1–10.

Conrad, M. E., & Umbreit, J. N. (2002). Pathways of iron absorption. *Blood Cells, Molecules, and Diseases, 29*, 336–355.

De Benoist, B., McLean, E., Egli, I., & Cogswell, M. (2008). *Worldwide prevalence of anaemia 1993–2005.* Geneva: WHO.

Di Battista, C. A., Constenla, D., Ramírez-Rigo, M. V., & Piña, J. (2015). The use of Arabic gum, maltodextrin and surfactants in the microencapsulation of phytosterols by spray drying. *Powder Technology, 286*, 193–201.

Ding, B., Zhang, X., Hayat, K., Xia, S., Jia, C., Xie, M., et al. (2011). Preparation, characterization and the stability of ferrous glycinate nanoliposomes. *Journal of Food Engineering, 102*(2), 202–208.

Dokic, P., Jakovljevic, J., & Dokic-Baucal, L. (1998). Molecular characteristics of maltodextrins and rheological behaviour of diluted and concentrated solutions. *Colloids and Surfaces A, 141*, 435–440.

Gharsallaoui, A., Roudaut, G., Chambin, O., Voilley, A., & Saurel, R. (2007). Applications of spray-drying in microencapsulation of food ingredients: An overview. *Food Research International, 40*, 1107–1121.

Gupta, C., Chawla, P., Arora, S., Tomar, S. K., & Singh, A. K. (2015). Iron microencapsulation with blend of gum Arabic, maltodextrin and modified starch using modified solvent evaporation method–milk fortification. *Food Hydrocolloids, 43*, 622–628.

Kenyon, M. M. (1995). Modified starch, maltodextrin, and corn syrup solids as wall materials for food encapsulation. In S. J. Risch, & G. A. Reineccius (Eds.). *Encapsulation and controlled release of food ingredients (pp. 42–50)*. Washington DC: American Chemical Society.

Kokkona, M., Kallinteri, P., Fatouros, D., & Antimisiaris, S. G. (2000). Stability of SUV liposomes in the presence of cholate salts and pancreatic lipases: Effect of lipid composition. *European Journal of Pharmaceutical Sciences, 9*, 245–252.

Kurozawa, L., Park, K., & Hubinger, M. (2009). Effect of Carrier agents on the physicochemical properties of a spray dried chicken meat protein hydrolysate. *Journal of Food Engineering, 94*, 326–333.

Li, Y., Diosady, L., & Wesley, A. (2010). Iodine stability in iodized salt dual fortified with microencapsulated ferrous fumarate made by an extrusion-based encapsulation process. *Journal of Food Engineering, 99*(2), 232–238.

Lim, W. T., & Nyam, K. L. (2016). Characteristics and controlled release behaviour of microencapsulated kenaf seed oil during in-vitro digestion. *Journal of Food Engineering, 182*, 26–32.

Lipiński, P., Stys, A., & Starzyński, R. (2013). Molecular insights into the regulation of iron metabolism during the prenatal and early postnatal periods. *Cellular and Molecular Life Sciences, 70*, 23–38.

Loksuwan, J. (2007). Characteristics of microencapsulated β-carotene formed by spray drying with modified tapioca starch, native tapioca starch and maltodextrin. *Food Hydrocolloids, 21*, 928–935.

Mishra, P., Mishra, S., & Mahanta, C. L. (2014). Effect of maltodextrin concentration and inlet temperature during spray drying on physicochemical and antioxidant properties of amla (*Emblica officinalis*) juice powder. *Food and Bioproducts Processing, 92*, 252–258.

Nedovic, V., Kalusevic, A., Manojlovic, V., Levic, S., & Bugarski, B. (2011). An overview of encapsulation technologies for food applications. *Procedia Food Science, 1*, 1806–1815.

Perez-Moral, N., Gonzalez, M., & Parker, R. (2013). Preparation of iron-loaded alginate gel beads and their release characteristics under simulated gastrointestinal conditions. *Food Hydrocolloids, 31*, 114–120.

Pizarro, F., Olivares, M., Valenzuela, C., Brito, A., Weinborn, V., Flores, S., et al. (2016). The effect of proteins from animal source foods on heme iron bioavailability in humans. *Food Chemistry, 196*, 733–738.

Ponka, P. (1999). Cell biology of heme. *The American Journal of the Medical Sciences, 318*(4), 241–256.

Santiago, R., Medina, L., Gallegos, J. A., Calderas, F., González, R. F., Rocha, N. E., et al. (2015). Spray drying-microencapsulation of cinnamon infusions (*Cinnamomum zeylanicum*) with maltodextrin. *LWT- Food Science and Technology, 64*, 571–577.

Thielbeer, F., Donaldson, K., & Bradley, M. (2011). Zeta potential mediated reaction monitoring on nano and microparticles. *Bioconjugate Chemistry, 22*, 144–150.

Tondeur, M., Schauer, C., Christofides, A., Asante, K., Newton, S., Serfass, R., et al. (2004). Determination of iron absorption from intrinsically labeled microencapsulated ferrous fumarate (sprinkles) in infants with different iron and hematologic status by using a dual-stable-isotope method. *American Journal of Clinical Nutrition, 80*, 1436–1444.

Tonon, R., Brabet, C., & Hubinger, M. (2008). Influence of process conditions on the physicochemical properties of açai (*Euterpe oleraceae* Mart.) powder produced by spray drying. *Journal of Food Engineering, 88*, 411–418.

Valenzuela, C., Hernández, V., Morales, S., Neira-Carrillo, A., & Pizarro, F. (2014). Preparation and characterization of heme iron-alginate beads. *LWT- Food Science and Technology, 59*, 1283–1289.

Valenzuela, C., Hernández, V., Morales, S., & Pizarro, F. (2016). Heme iron release from alginate beads at in vitro simulated gastrointestinal conditions. *Biological Trace Element Research, 172*, 251–257.

Vergote, G. J., Vervaet, C., Van Driessche, I., Hoste, S., De Smedt, S., Demeester, J., et al. (2001). An oral controlled release matrix pellet formulation containing nanocrystalline ketoprofen. *International Journal of Pharmaceutics, 219*, 81–87.

Viteri, F. (1997). Iron supplementation for the control of iron deficiency in populations at risk. *Nutrition Reviews, 55*, 195–209.

Wang, Y. J., & Wang, L. (2000). Structures and properties of commercial maltodextrins from corn, potato, and rice starches. *Starch Staerke, 52*, 296–304.

Wichchukit, S., Oztop, M. H., McCarthy, M. J., & McCarthy, K. L. (2013). Whey protein/alginate beads as carriers of a bioactive component. *Food Hydrocolloids, 33*, 66–73.

World Health Organization (WHO) (2015). *The global prevalence of anaemia in 2011.* Geneva: Switzerland, WHO.

Xu, Z., Liu, S., Wang, H., Gao, G., Yu, P., & Chang, Y. (2014). Encapsulation of iron in liposomes significantly improved the efficiency of iron supplementation in strenuously exercised rats. *Biological Trace Element Research, 162*, 181–188.

Yuan, L., Geng, L., Ge, L., Yu, P., Duan, X., Chen, J., et al. (2013). Effect of iron liposomes on anemia of inflammation. *International Journal of Pharmaceutics, 454*, 82–89.

Zariwala, M. G., Elsaid, N., Jackson, T. L., López, F. C., Farnaud, S., Somavarapu, S., et al. (2013). A novel approach to oral iron delivery using ferrous sulphate loaded solid lipid nanoparticles. *International Journal of Pharmaceutics, 456*(2), 400–407.

Zimmermann, M. B. (2004). The potential of encapsulated iron compounds in food fortification: A review. *International Journal for Vitamin and Nutrition Research, 74*, 453–461.

Zimmermann, M. B., & Hurrell, R. F. (2007). Nutritional iron deficiency. *The Lancet, 370*, 511–520.

Zlotkin, S. H., Schauer, C., Christofides, A., Sharieff, W., Tondeur, M. C., & Hyder, S. Z. (2005). Micronutrient sprinkles to control childhood anaemia. *PLoS Medicine, 2*(1), e1.